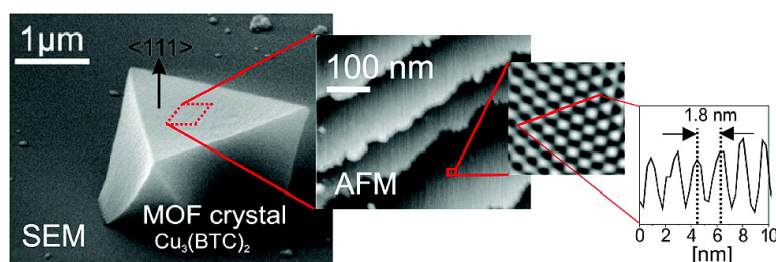Communication

Surface Structure of Metal#Organic Framework Grown on Self-Assembled Monolayers Revealed by High-Resolution Atomic Force Microscopy

Katarzyna Szelagowska-Kunstman, Piotr Cyganik, Maria Goryl, Denise Zacher, Zita Puterova, Roland A. Fischer, and Marek Szymonski

More About This Article

Additional resources and features associated with this article are available within the HTML version:

- Supporting Information
- Access to high resolution figures
- Links to articles and content related to this article
- Copyright permission to reproduce figures and/or text from this article

View the Full Text HTML

Surface Structure of Metal−Organic Framework Grown on Self-Assembled Monolayers Revealed by High-Resolution Atomic Force Microscopy

Katarzyna Szelagowska-Kunstman,[†] Piotr Cyganik,*[,†] Maria Goryl,[†] Denise Zacher,[‡] Zita Puterova,[§] Roland A. Fischer,[‡] and Marek Szymonski[†]

Research Center for Nanometer-Scale Science and Advanced Materials (NANOSAM), Faculty of Physics, Astronomy, and Applied Computer Science, Jagiellonian University, 30-059 Kraków, Poland, Organometallics and Materials Chemistry, Ruhr-University Bochum, D-44870 Bochum, Germany, and Department of Chemical Theory of Drugs, Faculty of Pharmacy, Comenius University, 832 32 Bratislava, Slovak Republic

Received September 3, 2008; E-mail: piotr.cyganik@uj.edu.pl

Metal−organic frameworks (MOFs) which consist of organic ligands linked together by metal ions belong to a relatively new class of porous materials. Owing to their potential applications in storage,[1] separation,[2] and heterogeneous catalysis,[3] MOFs have attracted increasing attention.[4,5] So far MOF research has been mainly focused on bulk structure of the material prepared in the form of a powder. Only very recently a new, and radically different, approach was undertaken by exploring the possibilities of MOF growth on surfaces in the form of thin films.[6−11] Two important aspects have been addressed by these studies. First, they demonstrated selective growth of MOFs on polar surfaces using differently functionalized self-assembled monolayers (SAMs) in combination with the microcontact printing technique.[6−10] Second, they proved the possibility of surface-oriented crystalline growth of the MOF structure.[8,11] Both achievements are technologically relevant since the first one demonstrates the possibility of spatial control of the MOF film architecture on the surface, and the second shows ability to control orientation of the crystals, and thus the pore system in such MOF films.

An important issue for further progress in optimizing growth of MOF crystals, and particularly MOF thin films, is control of their surface structure. Therefore, the high-resolution imaging of MOF surfaces by atomic force microscopy (AFM) is of key importance, as has been previously recognized for zeolites[12−14] which are analogous to MOFs. Only very recently was the first AFM study of a MOF crystal realized.[15] Although we also present an AFM study, we here propose a different and, in our opinion, more effective approach to surface analysis of MOFs. There are three important and new aspects introduced by the present paper. First, by performing analysis both in air and under ultra high vacuum (UHV) conditions for the first time high-resolution AFM imaging of a MOF surface is demonstrated. Second, for the first time the surface structure of a MOF crystal grown directly on the functionalized substrate is revealed and, moreover, this information is further utilized to optimize growth conditions. Finally, and most importantly, comparison of the present data with the previous ex situ AFM study[15] clearly demonstrates a much higher structural quality of MOF crystals grown on the substrate and, in contrast to the conventional method reported previously,[15] provides an experimentally convenient approach for in situ surface analysis of MOFs.

We have selected the $Cu_3(BTC)_2$ system (HKUST-1)[16] as a model case for our studies. It consists of Cu_2 units connected by BTC (1,3,5-benzenetricarboxylate) molecule in a paddle-wheel arrangement. The $Cu_3(BTC)_2$ microcrystals were grown on SiO_2/

† Jagiellonian University.
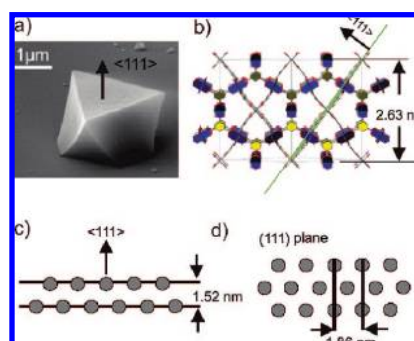‡ Ruhr-University Bochum.
§ Comenius University.

Figure 1. (a) SEM image of an individual $Cu_3(BTC)_2$ microcrystal grown on a COOH-terminated SiO_2/Si(100) substrate with an arrow showing the ⟨111⟩ direction perpendicular to the (111) crystal upper surface. (b) Schematic structure of the solvent free $Cu_3(BTC)_2$ crystal (based on the XRD data) with indicated cubic cell size of 2.63 nm and the (111) plane. (c−d) Simplified model of the fcc cubic structure of the $Cu_3(BTC)_2$ crystal showing the expected step height on the (111) surface (1.52 nm) and the size of the hexagonal structure in the (111) plane with a nearest neighbor distance of 1.86 nm.

Si(100) wafers functionalized by the COOH terminated SAMs following the procedure reported by us previously.[8] As documented by the X-ray diffraction data,[8] the growth of the $Cu_3(BTC)_2$ microcrystals directly from the solvothermal mother solution proceeds with the (111) crystal plane parallel to the substrate plane (Figure 1a−b). The AFM analysis was performed on the top (111) surface of an individual $Cu_3(BTC)_2$ microcrystal. The measurements were conducted both in air, using tapping mode (Nanoscope IIIa DI microscope), and in UHV using noncontact mode (VP2 Park Scientific microscope). Data obtained in air for the freshly prepared $Cu_3(BTC)_2$ crystal are presented in Figure 2a and show micrometer long terraces covered by much smaller depressions and islands with a diameter of 20−200 nm. The triangular shape of these features reflects the expected 3-fold symmetry the surface. The topographic profile (A) marked in Figure 2a shows that both islands and depressions correspond to the same change in height of about 1.5 nm which is fully consistent with expected height (1.52 nm) of steps on the (111) surface of the $Cu_3(BTC)_2$ crystal (Figure 1c). The observation of small depressions and islands exposing the last 2−4 layers of the crystal suggests that these features were created only at the very end of the crystal formation process, otherwise formation of large terraces would not have been possible. Since crystal formation takes place in the mother solution at elevated temperature (120 °C) followed by slow cooling to room temperature before the sample is removed for microscopic measurements, one can suppose that this slow cooling procedure is responsible for changing the crystal growth conditions and thus had an affect on
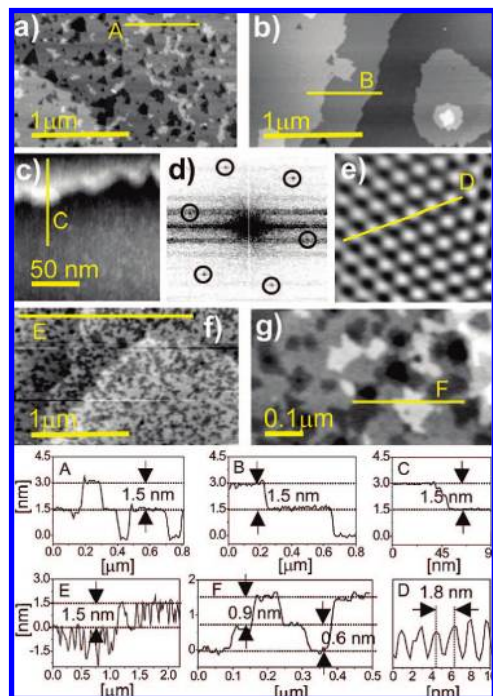
Figure 2. Upper part shows AFM images taken in air using tapping mode (a, b, f, g) and in UHV in noncontact mode (c) on the surface of Cu₃(BTC)₂ microcrystals prepared in different ways. (a) A fresh surface prepared by a standard procedure ending with slow cooling; (f, g) sample prepared by the same procedure but stored in air for 5 days before imaging; (b,c) a fresh surface prepared by a standard procedure followed by fast cooling; (d) FFT of the image shown in panel c; (e) part of panel c after filtering frequencies marked in panel d by circles. Lower part shows topographic profiles marked in images by yellow lines.

the last few layers of the MOF crystal structure. Following this idea we have analyzed samples directly removed from the hot mother solution. Typical AFM data are reproduced in Figure 2b and reveal a smooth surface (profile B) exhibiting micrometer long terraces which are completely free from any islands and depressions characteristic of crystals obtained by the slow cooling procedure. For such optimized surface structure of the MOF crystals we have conducted measurements in UHV using noncontact AFM which, in principle, enables analysis at molecular resolution. Although, collecting images with clearly visible molecular resolution was difficult, hexagonal periodicity with a distance of about 1.8 nm and orientation following high symmetry directions of the crystal could be seen reproducibly in the corresponding Fourier spectra (Figure 1d−e). These results are in full agreement with the expected (111) Cu₃(BTC)₂ surface structure (Figure 1d).

In the final experiments the influence of exposure to air of the Cu₃(BTC)₂ crystal surface was investigated. For this purpose a freshly prepared sample (the same as presented in Figure 2a) was imaged after storing it for 5 days in ambient conditions. The corresponding AFM data (Figure 2f) obtained in air show micrometer long terraces which exhibit an average height of 1.5 nm (profile E) and are covered by a very dense network of islands and depressions. Images collected at higher resolution (Figure 2g) show that, in contrast to freshly prepared sample, these features correspond to only a fraction of the complete layer of the Cu₃(BTC)₂ crystal structure, that is, about 0.6−0.9 nm as documented by the topographic profile (F). To confirm that this observation reflects the true topography of the sample and is not influenced by imaging

in ambient conditions (e.g., water condensation), the same sample was investigated also under UHV conditions using noncontact AFM after storing it for another 5 days in vacuum. The UHV experiment fully reproduced ambient results indicating that exposure to air induced erosion of the MOF surface. Considering the Cu₃(BTC)₂ crystal structure, as shown schematically in Figure 1b, we suppose that the observed fractional height corresponds to the loss of a BTC linker from the (111) surface and, effectively, to the local exposure of the (222) surface of the crystal.

The reported results are particularly satisfying when compared with the previous AFM study[15] for the (111) surface of the same Cu₃(BTC)₂ crystals prepared in the conventional way. The main observation emerging from the previous study was the very high density of screw dislocations and frequent fracturing which result in a high density of very short terraces (∼100 nm).[15] Moreover, as evidenced by the frequently observed steps with a height corresponding to the multiple of 1.52/2 height, this surface exhibits also (222) termination, which makes it chemically nonhomogenous.[15] In contrast, the crystals analyzed in our study were grown on the substrate and are essentially free from screw dislocation, and (after optimization of the preparation procedure) exhibit large micrometer-sized terraces with a homogeneous (111) termination (i.e., (222) termination was *only* observed as a result of surface erosion by long-term exposure to air). It is also crucial to note that the preparation of crystals suitable for an AFM study in previous studies required more then two years,[15] whereas, the crystals grown on the substrate reported here were prepared in just a few days.[8] Moreover, considering the very recent microwave-stimulated study of MOF growth on a substrate[17] this time could probably be shortened to a matter of minutes.

References

(1) Matsuda, R.; Kitaura, R.; Kitagawa, S.; Kubota, Y.; Belosludov, R. V.; Kobayashi, T. C.; Sakamoto, H.; Chiba, T.; Takata, M.; Kawazoe, Y.; Mita, Y. *Nature* **2005**, *436*, 238–241.
(2) Kawano, M.; Kawamichi, T.; Haneda, T.; Kojima, T.; Fujita, M. *J. Am. Chem. Soc.* **2007**, *129*, 15418–15419.
(3) Ohmori, O.; Fujita, M. *Chem. Commun.* **2004**, *14*, 1586–1587.
(4) Zaworotko, M. J. *Nature* **2008**, *451*, 410–411.
(5) Yaghi, O. M.; O'Keeffe, M.; Ockwig, N. W.; Chae, H. K.; Eddaoudi, M.; Kim, J. *Nature* **2003**, *423*, 705–714.
(6) Hermes, S.; Schröder, F.; Chelmowski, R.; Wöll, C.; Fischer, R. *J. Am. Chem. Soc.* **2005**, *127*, 13744–13745.
(7) Shekhah, O.; Wang, H.; Strunskus, T.; Cyganik, P.; Zacher, D.; Fischer, R. A.; Wöll, C. *Langmuir* **2007**, *23*, 7440–7442.
(8) Zacher, D.; Baunemann, A.; Hermes, S.; Fischer, R. A. *J. Mater. Chem.* **2007**, *17*, 2785–2792.
(9) Shekhah, O.; Wang, H.; Kowarik, S.; Schreiber, F.; Paulus, M.; Tolan, M.; Sternemann, C.; Evers, F.; Zacher, D.; Fischer, R. A.; Wöll, C. *J. Am. Chem. Soc.* **2007**, *129*, 15118–15119.
(10) Hermes, S.; Zacher, D.; Baunemann, A.; Woll, C.; Fischer, R. A. *Chem. Mater.* **2007**, *19*, 2168–2173.
(11) Biemmi, E.; Scherb, C.; Bein, T. *J. Am. Chem. Soc.* **2007**, *129*, 8054–8055.
(12) Agger, J. R.; Hanif, N.; Cundy, C. S.; Wade, A. P.; Dennison, S.; Rawlinson, P. A.; Anderson, M. W. *J. Am. Chem. Soc.* **2003**, *125*, 830–839.
(13) Meza, L. I.; Anderson, M. W.; Agger, J. R.; Cundy, C. S.; Chong, C. B.; Plaisted, R. J. *J. Am. Chem. Soc.* **2007**, *129*, 15192–15201.
(14) Roeffaers, M. B. J.; Ameloot, R.; Baruah, M.; Uji-i, H.; Bulut, M.; De Cremer, G.; Müller, U.; Jacobs, P. A.; Hofkens, J.; Sels, B. F.; De Vos, D. E. *J. Am. Chem. Soc.* **2008**, *130*, 5763–5772.
(15) Shôâeê, M.; Agger, J. R.; Anderson, M. W.; Attfield, M. P. *Crys. Eng. Comm.* **2008**, *10*, 646–648.
(16) Schlichte, K.; Kratzke, T.; Kaskel, S. *Microporous Mesoporous Mater.* **2004**, *73*, 81–88.
(17) Yoo, Y.; Jeong, H. K. *Chem. Commun.* **2008**, 2441–2443.

JA8069743